PERGAMON

International Journal of Solids and Structures 40 (2003) 361–384

INTERNATIONAL JOURNAL OF SOLIDS and STRUCTURES

www.elsevier.com/locate/ijsolstr

Electroelastic behavior modeling of piezoelectric composite materials containing spatially oriented reinforcements

N. Fakri [a], L. Azrar [a,*], L. El Bakkali [b]

[a] *Faculté des Sciences et Techniques de Tanger, Université Abdelmalek Essaadi, Laboratoire SDTAS, BP 416, Tanger, Morocco*
[b] *Faculté des Sciences de Tétouan, Université Abdelmalek Essaadi, Tétouan, Morocco*

Received 26 December 2001; received in revised form 2 September 2002

Abstract

In this work, a modeling of electroelastic composite materials is proposed. The extension of the heterogeneous inclusion problem of Eshelby for elastic to electroelastic behavior is formulated in terms of four interaction tensors related to Eshelby's electroelastic tensors. Analytical formulations of interaction tensors are presented for ellipsoidal inclusions. These tensors are basically used to derive the self-consistent model, Mori–Tanaka and dilute approaches. Numerical solutions are based on numerical computations of these tensors for various types of inclusions. Using the obtained results, effective electroelastic moduli of piezoelectric multiphase composites are investigated by an iterative procedure in the context of self-consistent scheme. Generalised Mori–Tanaka's model and dilute approach are reformulated and the three models are deeply analysed. Concentration tensors corresponding to each model are presented and relationships of effective coefficients are given. Numerical results of effective electroelastic moduli are presented for various types of piezoelectric inclusions and for various orientations and compared to existing experimental and theoretical ones.

Keywords: Micro-mechanics; Inclusion; Piezoelectric; Composite material; PZT; Self-consistent; Mori–Tanaka; Dilute; Effective electroelastic moduli; Interaction tensors; Concentration tensors; Orientation angles; Fiber; Ellipsoid

1. Introduction

Piezoelectric materials have the property of converting mechanical energy into electrical energy (direct piezoelectric effect) and vice versa (inverse piezoelectric effect). This electromechanical coupling behavior makes piezoelectric ceramics such as lead zirconium titanate (PZT) very attractive materials towards sensors, actuators and resonators applications. Some monolithic piezoelectric materials have, however, several drawbacks, namely in hydrostatic transducer applications. The low value of hydrostatic strain

* Corresponding author. Fax: +212-39-39-39-53.
E-mail address: azrar@hotmail.com (L. Azrar).

0020-7683/02/$ - see front matter
PII: S0020-7683(02)00524-3

coefficient limits their applicability. Hence, composite materials such as piezoelectric ceramic fibers embedded in a soft non-piezoelectric matrix are often a better technological solution for a lot of applications such as underwater and medical ultrasonic imaging (Challende, 1990) and transducers for underwater and sonar projector applications. They have superior electromechanical coupling characteristics (better acoustic impedance matching with water and (or) tissue) to conventional piezoelectric ceramic (Smith, 1989). Piezocomposites may provide material properties largely superior to conventional piezoelectric materials. For some years, materials science and engineering have been exploiting fibers to reinforce material. There is therefore a need for models that predict the electroelastic properties of such composites.

Several attempts to predict the effects of material properties and the micro-structural geometry of the constituents on the effective electroelastic behavior of composites were proposed. Firstly, Newnham et al. (1978) used a theory based on the idealized parallel and series connections of the constituents based on their three-dimensional connectivity characteristics for the analysis of the effective electroelastic moduli of piezoelectric composites. These analyses were extended by Banno (1983) to consider the effects of a discontinuous reinforcement through a "cubes" approach. Analytical predictions, primarily limited to unidirectional continuous fibers reinforced composite where one-dimensional analysis leads to adequate results, have been proposed by Smith and Auld (1991). However, in each of these approaches, simplifying assumptions have been made which led to the application of Voigt or Reuss type estimates (Chan and Unsworth, 1989). In more rigorous attempt to account for the interactions among continuous fibers at finite concentrations, Grekov et al. (1989) developed an extension of the well-known concentric cylinder models of elastic and electric behaviors, to coupled electroelastic behaviors in order to predict the effective electroelastic moduli of continuous fibers reinforced composites.

The analysis of piezoelectric composites with discontinuous reinforcement has received limited attention (Furukawa et al., 1976). An approach was proposed by Wang and Liu (1990) and Wang (1992) in which the coupled electroelastic field in piezoelectric ellipsoidal inhomogeneity embedded in an infinite matrix was developed. The obtained solution is expressed in terms of Fourier's transforms of electroelastic Green's functions. Explicit expressions for the effective electroelastic moduli of continuous fiber reinforced composites were derived by Wang (1992). However, this solution ignores the interaction among fibers that exist at finite concentrations and thus is valid only at dilute limit. The Wang's (1992) electroelastic fields are equivalent to those obtained by Deeg (1980) through a generalization of Eshelby's equivalent inclusion approach (Eshelby, 1957). The coupled electroelastic fields for the single ellipsoidal inclusion problem was obtained by Benveniste (1992) without giving any estimation of average fields. Based on the contour integral representation of Green's function derived by Deeg (1980); Dunn and Taya (1993b) made a significant contribution to the analysis of effective behavior of piezoelectric composites. Explicit expressions for a set of four tensors corresponding to Eshelby's elastic tensors are presented for ellipsoidal inclusions. They generalized several micro-mechanical models such as Mori and Tanaka's effective medium theory (Mori and Tanaka, 1973), dilute concentration approach, the differential scheme and self-consistent model. Estimations of the average electroelastic fields that exist at finite concentrations and predictions of the elastic, dielectric and piezoelectric moduli of two-phase composite materials reinforced by ellipsoidal particles or fibers are presented (Dunn and Taya, 1993b). Particular attention has been given by several authors to the Mori–Tanaka's method (Dunn and Taya, 1993a; Wang, 1994; Chen, 1994). Explicit closed-form expressions for the four analogous at Eshelby's tensors for spheroid inclusions in transversely isotropic piezoelectric medium are presented by Dunn and Wienecke (1997). More recently, the piezoelectric Eshelby's tensors for spheroidal inclusions are obtained explicitly by Mikata (2001). Huang and Kuo (1996) use the Mori–Tanaka's method to predict analytical expressions of effective electroelastic properties of composites in term of phase properties, orientation angles, volume fraction and inhomogeneity shape based on numerical computations of the four equivalent Eshelby's tensors. The finite element method to predict electroelastic constants in piezocomposites was used by several authors, namely, Poizat and Sester (1999) and Gaudenzi (1997).

In this work, an extension of the Eshelby's heterogeneous inclusion problem to electroelastic case is formulated by introducing four interaction tensors (Fakri and Azrar, 2001). An analytical formulation of interaction tensors is introduced and clearly presented for ellipsoidal inclusions. These tensors are basically used to derive the self-consistent model, Mori–Tanaka and dilute approaches. Numerical solutions are based on numerical computations of these tensors for various types of inclusions. Based on Fourier's transform and Gauss integration the resulting interaction tensors are numerically computed. Using the obtained results, average stress–electric displacement fields and effective electroelastic moduli of piezoelectric multiphase composites are investigated by an iterative procedure in the context of self-consistent scheme. The main assumption in this approach is that each inclusion is embedded in the effective medium of as yet unknown moduli. On the other hand, generalized Mori–Tanaka's model and dilute approach are reexamined using the four interaction tensors mentioned above to obtain effective electroelastic moduli of piezoelectric composites. The three models are deeply analyzed for various effective moduli and various types of piezoelectric inclusions. Numerical results of effective electroelastic coefficients are presented and compared to existing experimental and theoretical results.

2. Mathematical formulation

Let us consider a homogeneous piezoelectric material. In the stationary theory of linear piezoelectricity, the coupled interaction between the electrical and mechanical variables is expressed by the following relations:

$$\sigma_{ij} = C_{ijmn}\varepsilon_{mn} - e_{nij} \cdot E_n \tag{1}$$

$$D_i = e_{imn}\varepsilon_{mn} + \kappa_{in} \cdot E_n \tag{2}$$

Elastic strain, ε_{mn}, and electric field, E_n, are independent variables and related to stress, σ_{ij}, and electric displacement, D_i (see Ikeda (1990)). C_{ijmn}, e_{nij} and κ_{in} are the elastic moduli (measured in a constant electric field), the piezoelectric coefficients (measured at a constant strain or electric field) and the dielectric constants (measured at a constant strain) respectively. The strain and electric field are derivable from the elastic displacement vector u and electric potential Φ by the compatibility equation as

$$\varepsilon_{mn} = \frac{1}{2}(u_{m,n} + u_{n,m}) \tag{3}$$

$$E_n = -\Phi_{,n} \tag{4}$$

The stress and electric displacement fields should verify the equations of equilibrium, which in the absence of body forces and free charge are as follows:

$$\sigma_{ij,i} = 0 \tag{5}$$

$$D_{i,i} = 0 \tag{6}$$

The coupling between mechanic and electric variables is provided by the piezoelectric constants e_{nij}. Eqs. (1)–(6) constitute a set of 22 equations for the following 22 unknowns σ_{ij}, ε_{mn}, u_i, D_i, E_i and Φ.

In order to make easy the manipulation of these equations, the notation introduced by Barnett and Lothe (1975) is used. This notation is identical to the conventional subscripts notations with the exception that lower case subscripts take on the range 1–3, while capital subscripts take on the range 1–4 and repeated capital subscripts are summed over 1–4. With this notation, the elastic-strain-electric field Z_{Mn} is expressed as

$$Z_{Mn} = \begin{cases} \varepsilon_{mn} & M = 1,2,3 \\ -E_n & M = 4 \end{cases} \tag{7}$$

Z_{Mn} is derivable from elastic displacement–electric potential field U_M given by

$$U_M = \begin{cases} u_m & M = 1,2,3 \\ \Phi & M = 4 \end{cases} \tag{8}$$

Similarly, the stress–electric displacement Σ_{iJ} is represented by

$$\Sigma_{iJ} = \begin{cases} \sigma_{ij} & J = 1,2,3 \\ D_i & J = 4 \end{cases} \tag{9}$$

The electroelastic moduli can then be represented as follows:

$$E_{iJMn} = \begin{cases} C_{ijmn} & J = 1,2,3; \quad M = 1,2,3 \\ e_{nij} & J = 1,2,3; \quad M = 4 \\ e_{imn} & J = 4; \quad M = 1,2,3 \\ -\kappa_{in} & J = 4; \quad M = 4 \end{cases} \tag{10}$$

The symmetry properties of E_{iJMn} derive from those of C_{ijmn}, e_{nij} and κ_{in}. With these shorthand notations, (1) and (2) can be unified into a single shorthand equation

$$\Sigma_{iJ} = E_{iJMn} Z_{Mn} \tag{11}$$

This equation is reduced to the well-known Hooke's law in elastic case.

Let us recall that Z_{Mn}, U_M, Σ_{iJ} and E_{iJMn} are not tensors. It is often convenient to use the matrix notations. These parameters can then be written in the following form:

$$E_{iJMn} = \begin{bmatrix} C_{ijmn} & e^t_{nij} \\ e_{imn} & -\kappa_{in} \end{bmatrix} \quad Z_{Mn} = \begin{bmatrix} \varepsilon_{mn} \\ -E_n \end{bmatrix} \quad \Sigma_{iJ} = \begin{bmatrix} \sigma_{ij} \\ D_i \end{bmatrix} \tag{12}$$

C, e and κ are elastic, piezoelectric and dielectric coefficients respectively. Then the electroelastic coefficients can be represented by the (9×9) matrix E. Similarly, Z and Σ are represented by the (9×1) matrices. Thus, to write the equations, each individual tensor must be transformed by the well known laws of tensor transformations. The resulting tensors can then be reunified into the form of (7) to (10). Substituting Eqs. (3) and (4) into Eqs. (1) and (2) and considering the symmetries, one can get

$$\Sigma_{iJ} = E_{iJMn} U_{M,n} \tag{13}$$

Introducing this equation in shorthand notations of Eqs. (5) and (6), the following partial derivative equations is obtained:

$$(E_{iJMn} U_{M,n}), \quad i = 0 \tag{14}$$

3. Generalized integral equation

In this section, the expression of the local strain field based on integral equations proposed by Dederish and Zeller (1973) for elastic case is extended, to electroelastic case. The resulting local strain and electric fields are expressed with generalized integral equations. An infinite media with a linear electroelastic behavior is considered. Introducing a homogeneous fictive media called "reference media", with electroelastic moduli E^0, the local electroelastic moduli can then be written as

$$E_{iJMn}(r) = E^0_{iJMn} + \delta E_{iJMn}(r) \tag{15}$$

in which 'r' is the position vector in the considered media and $\delta E(r)$ is the deviation. The introduction of Eq. (15) into the equilibrium Eq. (14) leads to

$$E^0_{iJMn}U_{M,ni}(r) + (\delta E_{iJMn}(r)U_{M,n}(r)), \quad i = 0 \tag{16}$$

Let us introduce the electroelastic Green's functions denoted by $G_{MJ}(r - r')$ of the "reference media" as defined by Deeg (1980) relate response at the position $\mathbf{r}$ due to a unit point force or charge at $\mathbf{r}'$ (see Appendix B). These tensors must satisfy the following differential equations (Dunn, 1994):

$$E^0_{iJMn}G_{MK,in}(r - r') + \delta_{JK}\delta(r - r') = 0 \tag{17a}$$

where $\delta(r - r')$ is the three-dimensional Dirac delta function and δ_{JK} is the generalized Krönecker delta. These equations can be expressed explicitly as

$$C^0_{ijmn}G_{mk,in} + e^{0t}_{nij}G_{4k,in} + \delta_{jk}\delta(r - r') = 0 \tag{17b}$$

$$e^0_{imn}G_{m4,in} - \kappa^0_{in}G_{44,in} + \delta(r - r') = 0 \tag{17c}$$

$$e^0_{imn}G_{mk,in} - \kappa^0_{in}G_{4k,in} = 0 \tag{17d}$$

$$C^0_{ijmn}G_{m4,in} + e^{0t}_{nij}G_{44,in} = 0 \tag{17e}$$

On the other hand, the elastic displacement and electric potential, represented by U_M, are formulated as

$$U_K(r) = \int_V U_M(r')\delta_{MK}\delta(r - r')\,\mathrm{d}V' \tag{18}$$

After some manipulations and consideration of boundary conditions, the expression of $U_K(r)$, developed in Appendix A, can be expressed as

$$U_K(r) = U^0_K(r) + \int_V G_{JK}(r - r')(\delta E_{iJMn}(r')U_{M,n}(r'))_{,i'}\,\mathrm{d}V' \tag{19}$$

in which U^0_K is the displacement–electric potential of an homogeneous medium, with an equivalent geometry and boundaries conditions as considered medium.

Considering the fact that Z_{Kl} is derivable from U_K (see Eqs. (3), (4), (7) and (8)), Z_{Kl} can be expressed by

$$Z_{Kl} = U_{K,L} \tag{20}$$

Then $Z_{Kl}(r)$ can be obtained as

$$Z_{Kl}(r) = Z^0_{Kl} + \int_V G_{JK,l}(r - r')(\delta E_{iJMn}(r')Z_{Mn}(r'))_{,i'}\,\mathrm{d}V' \tag{21}$$

After integrating by parts the above equation and considering that the strain-electric field vanishes at the boundaries, $Z_{Kl}(r)$ can be expressed as

$$Z_{Kl}(r) = Z^0_{Kl} - \int_V G_{JK,li'}(r - r')\delta E_{iJMn}(r')Z_{Mn}(r')\,\mathrm{d}V' \tag{22}$$

Let us recall that the partial differentiation ($\partial_i = -\partial_{i'}$) and introduce fours tensors represented by the following shorthand expression:

$$\Gamma_{iJKl}(r - r') = -G_{JK,li}(r - r') \tag{23}$$

The explicit expression of $\Gamma_{iJKl}(r-r')$ is

$$\begin{aligned}
&-\frac{1}{2}\left(G_{jk,li}(r-r')+G_{jl,ki}(r-r')\right) && \text{for } J \text{ and } K=1,2,3\\
&-\frac{1}{2}\left(G_{4k,li}(r-r')+G_{4l,ki}(r-r')\right) && \text{for } J=4 \text{ and } K=1,2,3\\
&-G_{J4,li}(r-r') && \text{for } J=1,2,3 \text{ and } K=4\\
&-G_{44,li}(r-r') && \text{for } J=4 \text{ and } K=4
\end{aligned}$$

Finally, the strain-electric field is given by the following integral equation:

$$Z_{Kl}(r)=Z^0_{Kl}-\int_V \Gamma_{iJKl}(r-r')\delta E_{iJMn}(r')Z_{Mn}(r')\,\mathrm{d}V' \tag{24}$$

This equation is an implicit expression of strain-electric fields $Z_{Kl}(r)$. To obtain the solution of this equation, a methodology based on equivalent inclusion problem is developed and used in this paper. This leads to equations of localization relating Z_{Kl} (local field) and Z^0_{Kl} (macroscopic field) by means of concentration factors. Then the solution of the integral equation (24) is the key of the localization problem for micro-heterogeneous media.

4. Solutions of the integral equation

4.1. Equivalent inclusion problem

Considering an infinite medium with electroelastic moduli E^0_{iJMn} which contains a single inclusion "I" with a volume V^I and electroelastic moduli E^I_{iJMn} constant inside the volume V^I, the inhomogeneity can be simulated by an "equivalent inclusion". Based on these assumptions, as shown by Eshelby (1957) in the elastic case and by Deeg (1980) in electroelastic case, one can get

$$\delta E_{iJMn}(r)=(E^I_{iJMn}-E^0_{iJMn})\theta^I(r)$$

or

$$\delta E_{iJMn}(r)=\Delta E^I_{iJMn}\theta^I(r) \tag{25}$$

where $\theta^I(r)$ is the characteristic function of V^I ($\theta^I(r)$ equals to '1' inside of V^I and to '0' outside of V^I). Based on Eq. (24), the average of the strain-electric field Z^I_{Kl} in the considered inclusion is calculated by

$$Z^I_{Kl}=Z^0_{Kl}-\frac{1}{V^I}\int_{V^I}\int_V \Gamma_{iJKl}(r-r')\Delta E^I_{iJMn}\theta^I(r')Z_{Mn}(r')\,\mathrm{d}V'\,\mathrm{d}V \tag{26}$$

Exact solutions of this equation are difficult to obtain. An approximate solution based on the effective field method can be obtained replacing $Z_{Mn}(r')$ by the average value Z^I_{Kl} in the inclusion as follows:

$$Z^I_{Kl}=Z^0_{Kl}-\frac{1}{V^I}\int_{V^I}\int_{V^I} \Gamma_{iJKl}(r-r')\Delta E^I_{iJMn}Z^I_{Mn}\,\mathrm{d}V'\,\mathrm{d}V \tag{27}$$

This equation can be formulated in the following form:

$$Z^I_{Kl}=Z^0_{Kl}-\frac{1}{V^I}T^{II}_{iJKl}\Delta E^I_{iJMn}Z^I_{Mn} \tag{28}$$

$$T^{II}_{iJKl}=\int_{V^I}\int_{V^I}\Gamma_{iJKl}(r-r')\,\mathrm{d}V'\,\mathrm{d}V \tag{29}$$

T^{II}_{iJKl} represent four interaction tensors and explicit expressions of these tensors are elaborated in Appendix B. T^{II}_{iJKl} are related to electroelastic Eshelby's tensors, "S_{iJKl}", used by Dunn and Taya (1993a), by the following relationship:

$$S_{JiMn} = E^0_{lKMn} T^{II}_{iJKl} \tag{30}$$

In the elastic case, the last tensors are reduced to the well known Eshelby's tensor S_{jimn} (Eshelby, 1957).

In many published papers on piezoelectric composites, the tensors S_{IjKl} are used. These tensors and Green's functions are analytically computed for simple shapes of inclusions by some authors. Mikata (2001) recently presents an explicit determination of piezoelectric Eshelby's tensors for spherical inclusions. In the present work, a general ellipsoidal inclusion in transversely isotropic piezoelectric solid is considered. An analytical formulation of the interaction tensors, T^{II}_{iJKl}, is clearly presented. Numerical solutions are based on numerical computation of tensors T^{II}_{iJKl} for various types of inclusions.

4.2. The self-consistent approximation

In order to give a solution of integral equation (27) based on equivalent inclusion problem, the self-consistent method will be used here. This will permit to take into account the interactions existing between inclusion and matrix for predictions of effective electroelastic moduli of non-piezoelectric materials reinforced by piezoelectric fibers or particles. The self-consistent model initially investigated by Hershey (1954) and Kröner (1958) for polycrystalline aggregate with a linear behavior consists in considering one single heterogeneity (inclusion) embedded in an homogeneous medium (matrix) with effective electroelastic moduli E^{eff}_{iJMn} not yet known and taking into account the equivalent behavior of neighboring medium of inclusion. In contrast with the last case, the heterogeneity was embedded in homogeneous medium with electroelastic moduli E^0_{iJMn}. Under these conditions the expression of the field Z^I becomes

$$Z^I_{Kl} = Z_{Kl} - \frac{1}{V^I} T^{II}_{iJKl} \Delta E^I_{iJMn} Z^I_{Mn} \tag{31}$$

$$\Delta E^I_{iJMn} = E^I_{iJMn} - E^{\text{eff}}_{iJMn} \tag{32}$$

where Z_{Kl} is the macroscopic homogeneous strain-electric field obtained by the average of $Z_{Kl}(r)$ over the total volume of medium and compatible with boundary conditions

$$Z_{Kl} = \frac{1}{V} \int_V Z_{Kl}(r)\, \mathrm{d}V \tag{33}$$

in which V is the total volume of medium (inclusion + matrix).

The final expression of the local field Z^I as a function of global or macroscopic fields Z_{Kl} is then

$$Z^I_{Mn} = \left(I_{KlMn} + \frac{1}{V^I} T^{II}_{iJKl} \Delta E^I_{iJMn} \right)^{-1} Z_{Kl} \tag{34}$$

or

$$Z^I_{Mn} = A^{\text{Sc}}_{MnKl} Z_{Kl} \tag{35}$$

A^{Sc}_{MnKl} is the shorthand notation of four concentration tensors. Explicit expressions of these tensors are presented in Appendix C.

For an N-phase medium the average definition of the stress and electric displacement $\bar{\Sigma}_{iJ}$ can be expressed, since Hill-Mandel average formulation, in the following form:

$$\bar{\Sigma}_{iJ} = \sum_{I=1}^{N} f^I E^I_{iJMn} Z^I_{Mn} \tag{36}$$

where $f^I = \frac{V^I}{V}$ is the concentration of the inclusion I.

Substituting (35) into (36) one can obtain

$$\bar{\Sigma}_{iJ} = \sum_{I=1}^{N} f^I E^I_{iJMn} A^{\mathrm{Sc}}_{MnKl} Z_{Kl} \tag{37}$$

Namely, Z_{Mn} is a constant strain-electric field, then it can be taken out of the summation symbol. Finally, the effective electroelastic moduli, E^{eff}, obtained by the self-consistent model can be expressed by

$$E^{\mathrm{eff}}_{iJKl} = \sum_{I=1}^{N} f^I E^I_{iJMn} A^{\mathrm{Sc}}_{MnKl} \tag{38}$$

If the first phase ($N = 1$) is considered as matrix (symbol "m"), the last expression becomes

$$E^{\mathrm{eff}}_{iJKl} = E^{\mathrm{m}}_{iJKl} + \sum_{I=2}^{N} f^I (E^I_{iJMn} - E^{\mathrm{m}}_{iJMn}) A^{\mathrm{Sc}}_{MnKl} \tag{39}$$

Let us recall that $\sum_{I=1}^{N} f^I A^{\mathrm{Sc}}_{MnKl} = I_{MnKl}$, where I_{MnKl} is the shorthand notation for the fourth order and second order identity tensors (Dunn and Taya (1993a))

$$I_{MnKl} = \begin{cases} I_{mnkl} & K, M = 1, 2, 3 \\ 0 & K = 1, 2, 3;\ \ M = 4 \\ 0 & K = 4;\ \ M = 1, 2, 3 \\ I_{nl} & K = 4;\ \ M = 4 \end{cases} \tag{40}$$

E^{m}_{iJKl} correspond to matrix electroelastic moduli and E^I_{iJMn} correspond to inclusion electroelastic moduli. These formulations permit one to predict the effective electroelastic moduli for N-phase composites. For a two-phase composites the expression of E^{eff}_{iJKl} becomes

$$E^{\mathrm{eff}}_{iJKl} = E^{\mathrm{m}}_{iJKl} + f^I (E^I_{iJMn} - E^{\mathrm{m}}_{iJMn}) A^{\mathrm{Sc}}_{MnKl} \tag{41}$$

Let us recall that equations (39) and (41) give coupled and implicit expressions of the effective electroelastic moduli of piezoelectric material. The concentration factors A^{Sc} are functions of E^{eff}. This kind of equations is generally solved by iterative methods, which need a starting solution. The initial values of E^{eff} may be those of Voigt generalized approximations as in the present work

$$E^V_{iJKl} = \sum_I f^I E^I_{iJMn} I_{MnKl} \tag{42}$$

Additionally, the concentration factors A^{Sc}, in the expression of E^{eff}, depend on T^{II} which need to be firstly computed. The tensors T^{II} are obtained by Fourier's transforms of the Green's functions and numerical evaluation of integrals are investigated. After computing the tensors T^{II} with the electroelastic starting solution obtained by Voigt approximation (42), it is introduced in the formulation of concentration factors A^{Sc} in order to get the first value of effective electroelastic moduli E^{eff}_1. This operation is repeated until convergence of the method. The algorithm describing this methodological approach is presented in Appendix D.

4.3. Generalized Mori–Tanaka approach

In this approach, the interaction between matrix and inclusion is taken into account by considering a finite concentration of inclusions embedded in an infinite matrix with electroelastic moduli E^I_{iJKl} and E^{m}_{iJKl} respectively and subjected to electroelastic uniform field Z^0 at boundaries. The interaction matrix-inclusion is restricted in the effect of concentration of inclusion. In this approach, the expression of strain-electric fields Z^I_{Kl} is similar to that derived by the self-consistent approach but more simplified considering the fact that in this case the term E^{eff}_{iJMn} in Eq. (34) (see (32) again) is replaced by E^{m}_{iJMn} in the term ΔE^I_{iJMn}. Then, the expression becomes explicit and the computation is straightforward. Additionally, the term $\frac{1}{V^I}$ is replaced by $\frac{f^{\mathrm{m}}}{V^I}$, where f^{m} is concentration of matrix. The expression of strain-electric field for Mori–Tanaka's approximation is then

$$Z^I_{Mn} = \left(I_{KlMn} + \frac{f^{\mathrm{m}}}{V^I} T^{II}_{iJKl} \Delta E^I_{iJMn} \right)^{-1} Z^0_{Kl} \tag{43}$$

in which Z^0 are also here macroscopic strain-electric fields of equivalent homogeneous medium. The concentration tensors A^{MT}, corresponding to Mori–Tanaka's model, are then expressed as

$$A^{MT}_{MnKl} = \left(I_{KlMn} + \frac{f^{\mathrm{m}}}{V^I} T^{II}_{iJKl} \Delta E^I_{iJMn} \right)^{-1} \tag{44}$$

Similarly to the self-consistent approach, the effective behavior for two-phase composites can be obtained by

$$E^{\mathrm{eff}}_{iJKl} = E^{\mathrm{m}}_{iJKl} + f^I (E^I_{iJMn} - E^{\mathrm{m}}_{iJMn}) A^{MT}_{MnKl} \tag{45}$$

4.4. Dilute approach

This approach has equivalent scheme than the above approaches but does not consider any interaction between the infinite matrix and the embedded single inclusion. Then the expression of strain-electric fields Z^I_{Kl} of inclusion can be derived from that obtained in self-consistent approach with the difference that in this case, the infinite matrix has electroelastic moduli E^{m} as equivalent behavior. Than, the expression of strain-electric field in inclusion is obtained as follows:

$$Z^I_{Mn} = \left(I_{KlMn} + \frac{1}{V^I} T^{II}_{iJKl} \Delta E^I_{iJMn} \right)^{-1} Z^0_{Kl} \tag{46}$$

namely, $\Delta E^I_{iJMn} = E^I_{iJMn} - E^{\mathrm{m}}_{iJMn}$.

Z^0_{Mn} also here is the macroscopic strain-electric field of an equivalent homogeneous medium. The concentration factors A^{Dil}, corresponding to dilute approach, have the following expression:

$$A^{\mathrm{Dil}}_{MnKl} = \left(I_{KlMn} + \frac{1}{V^I} T^{II}_{iJKl} \Delta E^I_{iJMn} \right)^{-1} \tag{47}$$

Finally the effective behavior in this case is expressed as

$$E^{\mathrm{eff}}_{iJKl} = E^{\mathrm{m}}_{iJKl} + f^I (E^I_{iJMn} - E^{\mathrm{m}}_{iJMn}) A^{\mathrm{Dil}}_{MnKl} \tag{48}$$

5. Numerical results

In this section, "Ceramic-Polymer" composites are considered. The first phase, matrix, is constituted of spherical inclusions of isotropic polymer. The second phase, reinforcement, is a transversely isotropic

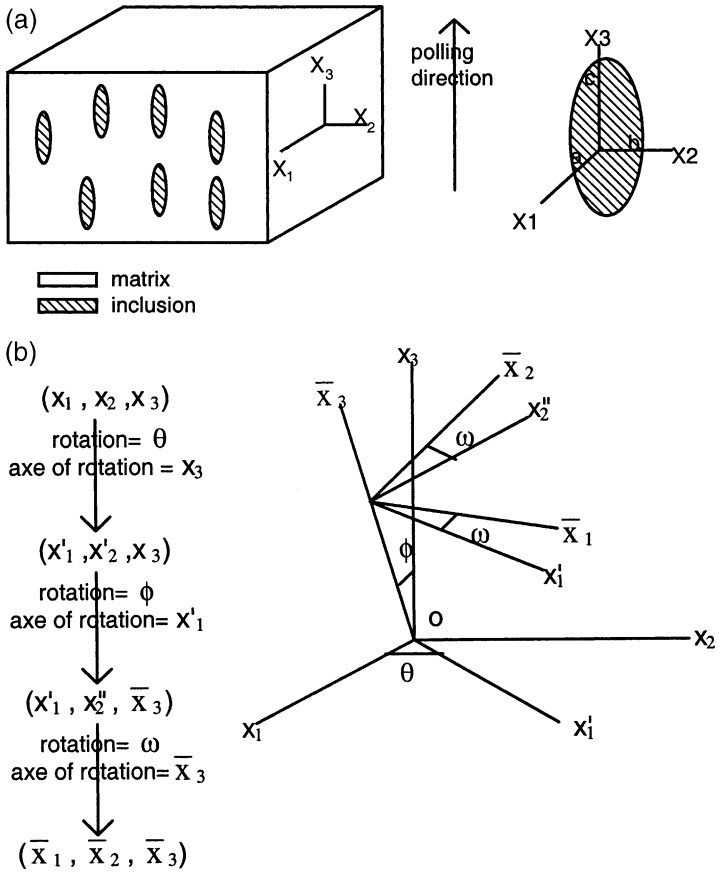

Fig. 1. (a) Scheme of spatial distribution of inclusions which third half axe "c" is aligned with polling and global direction x_3. (b) Definition of Euler angles θ, ϕ and ω.

ellipsoidal inclusions of ceramic with half axes a, b and c. The global coordinate system related to matrix is (x_1, x_2, x_3) and the third half axe "c" of inclusion is respected with the polling direction x_3 (see Fig. 1a). Namely a spatial orientation of inclusion in generally anisotropic medium can be described by three Euler angles θ, ϕ and ω (Fig. 1b). Let u_1, u_2 and u_3 be unit vectors in the (x_1, x_2, x_3), global coordinate system and $\bar{u}_1$, $\bar{u}_2$, $\bar{u}_3$ be the unit vector in $(\bar{x}_1, \bar{x}_2, \bar{x}_3)$ coordinate system related to inclusion. The relationship between these two unit vectors can be expressed as

$$\begin{Bmatrix} \bar{u}_1 \\ \bar{u}_2 \\ \bar{u}_3 \end{Bmatrix} = [\Psi] \begin{Bmatrix} u_1 \\ u_2 \\ u_3 \end{Bmatrix} \tag{49}$$

$$[\Psi] = \begin{bmatrix} mr - spn & rn + spm & sn \\ -rpn - sm & rpm - sn & rq \\ qn & -qm & p \end{bmatrix}$$

where $[\Psi]$ is the direction cosine matrix, $m = \cos\theta$, $n = \sin\theta$, $p = \cos\phi$, $q = \sin\phi$, $r = \cos\omega$ and $s = \sin\omega$.

In the first part of the present work, the principal axes of the ellipsoid coincide with the global coordinate system. In this particular case, the Euler angles vanish ($\theta = \phi = \omega = 0$). Let us precise that the models

presented in the last paragraphs, used for predictions of electroelastic coefficients, can be easily used for all inclusion spatial orientations and multi-phase composites. The micro-mechanical approaches presented above are applied for different composites to predict effective electroelastic moduli E^{eff}_{iJMn}. Additionally from the symmetry of C_{ijmn}, e_{nij} and κ_{in}, it can be seen that the (9×9) matrix E^{I}_{iJKl} possesses a diagonal symmetry. In a similar manner, E^{eff}_{iJMn} can also be shown to possess a diagonal symmetry and has shape of transversely isotropic materials electroelastic (9×9) matrix. The electroelastic moduli of the constituents used in our investigation are given in Table 1. These values are obtained from the following papers Berlincourt (1971); Chan and Unsworth (1989) and Huang (1995). The well-known Voigt two index notation is adopted.

The aim of this study is primarily to clarify the effect of inclusion shapes and orientations and to identify the predictions of the three presented models for various effective parameters. It is well know that, for fibers inclusions, the predictions of piezoelectric strain coefficient d_{33} based on the three micro-mechanical models, dilute, Mori–Tanaka and self-consistent, are indistinguishable for the composites PZT-7A*/epoxy-1, as presented by Dunn and Taya (1993b). Based on the three models presented above, Fig. 2 illustrates numerical results obtained for PZT-7A*/epoxy-1 composite. The obtained results are the same than those presented by Dunn and Taya and by various authors (Poizat and Sester, 1999; Jiang et al., 1999; Kreher,

Table 1
Electroelastic material properties

	C_{11} (GPa)	C_{12} (GPa)	C_{13} (GPa)	C_{33} (GPa)	C_{44} (GPa)	e_{31} (C/m^2)	e_{33} (C/m^2)	e_{15} (C/m^2)	κ_{11}/κ_0[a]	κ_{33}/κ_0[a]
PZT-7A	148	76.2	74.2	131	25.4	−2.1	9.5	9.2	460	235
PZT-7A*	148	76.2	74.2	131	25.4	−2.1	12.3	9.2	460	235
PZT-5	121	75.4	75.2	111	21.1	−5.4	15.8	12.3	916	830
PZT-4	139	77.8	74.3	115	25.6	−5.2	15.1	12.7	730	635
$BaTiO_3$	166	77	78	162	43	−4.4	18.6	11.6	1665.5	1423.7
Epoxy-1	8.0	4.4	4.4	8.0	1.8	0	0	0	4.2	4.2
Epoxy-2	6.43	4.29	4.29	6.43	1.07	0	0	0	5	5

[a] $\kappa_0 = 8.85 \times 10^{-12}$ (C^2/Nm^2) = permittivity of free space.

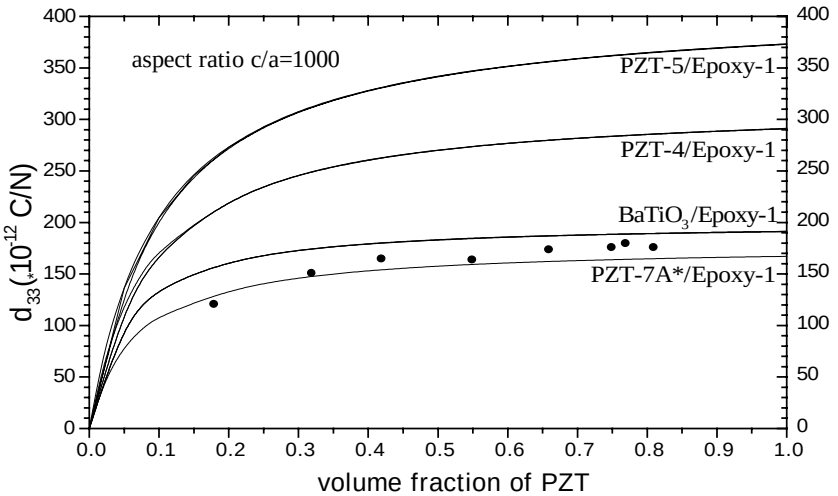

Fig. 2. Effective piezoelectric module d_{33} predicted by self consistent model, Mori–Tanaka and dilute approaches for several ceramic continuous fibers $(c/a = 1000)$ reinforced epoxy composites as a function of fibers concentration. "●" indicate experimental results (Chan and Unsworth, 1989) for PZT-7A*/epoxy composite compared to computed results.

1998) and are in good agreement with the experimental results of Chan and Unsworth (1989). Our aim here is to analyze if these three models give similar predictions for other fiber inclusions. It is clearly shown in Fig. 2 that for PZT-5/epoxy-1, PZT-4/epoxy-1 and $BaTiO_3$/epoxy-1, the three models lead to the same predictions for each composite for this kind of inclusions (fibers $c/a = 1000$). It can be remarked that the evolution of d_{33} with concentration of all ceramic fibers presents a strong variation at the small concentration near to 0.2 and a very low variation over. In Fig. 3, numerical results for the piezoelectric strain coefficient d_{33} are plotted against the concentration of PZT-7A* reinforcement and compared with numerical results of Kreher (1998) using the effective field approach (EFA). The used composite is epoxy-1 reinforced by long and short fibers and spherical particles. The three micro-mechanical models, dilute, Mori–Tanaka and self-consistent are used for computation. It can be seen that for long fibers, as in Fig. 2, the three micro-mechanical models predictions are indistinguishable and agree with numerical results presented by Kreher (1998). In contrast with the case of short fibers and particles (aspect ratio $c/a = 10$ and 1), The three models give different results. Self-consistent model gives high values of d_{33} than Mori–Tanaka and dilute models for $(c/a = 10)$ and $(c/a = 1)$. It is clearly shown that the dilute model doesn't predict acceptable result at high concentration limit $(f^I = 1)$ and appears to be an asymptotic limit of Mori–Tanaka's approximation for small concentrations. The results taken from a curve of Kreher (1998) obtained by EFA are reported in Fig. 3 and are similar to those obtained by the presented Mori–Tanaka's approach. This similarity is expected because Mori–Tanaka's model seems to be a particular case of the EFA. An interesting conclusion from this figure is that d_{33} computed by self-consistent method becomes nearly insensitive towards reinforcement shape in contrast with dilute, Mori–Tanaka models and Effective Field Approximation (Kreher, 1998) for which d_{33} is strongly affected by reinforcement shape. Fig. 4 show the variation of numerically predicted piezoelectric coefficients e_{33} and e_{31} for PZT-7A/epoxy-1 composite varied with concentration of PZT-7A for different aspect ratios of inclusions. It can be seen also from Fig. 4a that the predictions of e_{33} by the three models, self-consistent, Mori–Tanaka and dilute, are the same for long fibers inclusions. But for spherical inclusions (Fig. 4b), the predictions of self-consistent scheme are

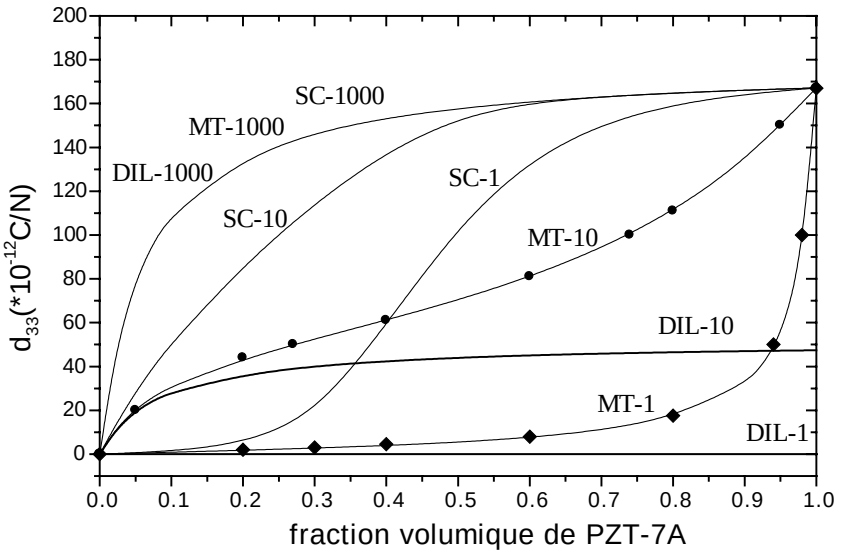

Fig. 3. Comparison of micro-mechanical predictions of effective piezoelectric moduli d_{33} of PZT-7A* continuous fibers $(c/a = 1000)$, ellipsoids $(c/a = 10)$, and particles $(c/a = 1)$ reinforced epoxy composite as a function of reinforcement volume fractions. SC: self-consistent; MT: Mori–Tanaka; DIL: dilute. "●" and "◆": EFA results from a curve of Kreher (1998).

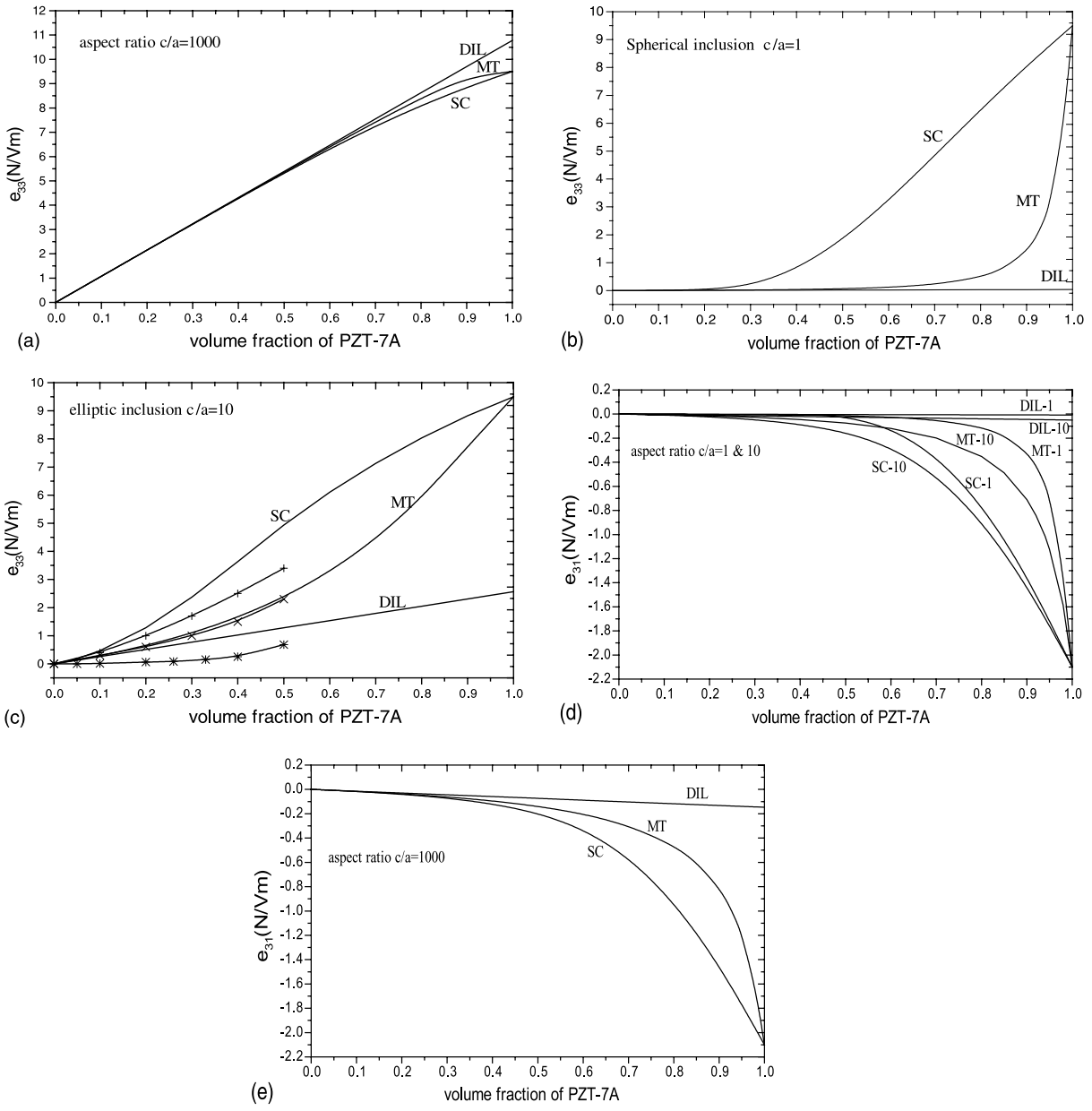

Fig. 4. (a) Effective piezoelectric moduli e_{33} of PZT-7A long fibers $(c/a = 1000)$ reinforced epoxy-1 composite as a function of fiber volume fraction. (b) Effective piezoelectric moduli e_{33} of PZT-7A spherical particles $(c/a = 1)$ reinforced epoxy-1 composite as a function of fiber volume fraction. (c) Effective piezoelectric moduli e_{33} of PZT-7A elliptical fibers $(c/a = 10)$ reinforced epoxy-1 composite as a function of fiber volume fraction. Comparison with numerical results obtained from Fig. 5 of (Poizat and Sester, 1999). "*": FE-unit cell method (simple cubic); "×": EFA; "+": FE-unit cell method (body centered cubic). (d) Effective piezoelectric moduli e_{31} of PZT-7A spherical particles and ellipsoidal fibers $(c/a = 1$ and $10)$ reinforced epoxy-1 composite as a function of fibers (particles) volume fraction. (e) Effective piezoelectric moduli e_{31} of PZT-7A long fibers $(c/a = 1000)$ reinforced epoxy-1 composite as a function of fiber volume fraction.

overestimated than those of the other two models. Fig. 4c illustrates the numerical results computed by the three models mentioned above and compared with those obtained by (Poizat and Sester, 1999) using finite element method and EFA for concentrations of piezoelectric inclusions low than 0.5. It can be seen again that results obtained by the presented Mori–Tanaka's approach agree well with the EFA predictions. The self-consistent scheme, which is usually criticized for large volume fractions and particularly for spherical inclusions, leads to good qualitative results in comparison with the FE unit cell method based on body centered cubic. But, the FE unit cell method using simple cubic lattice leads to erroneous results in comparison with the other models as can be shown in the Fig. 4c.

In contrast with e_{33}, the piezoelectric coefficient e_{31} predicted by the three models seems to be insensitive to shape of inclusions and the models lead to distinguished results for all shapes of inclusions (see Fig. 4d and e). We clearly demonstrate by these curves that even if the inclusions are long fibers ($c/a = 1000$), for which the prediction of the three models coincide perfectly for d_{33}, there are discrepancies for other predicted coefficients. For fiber inclusions, this discrepancy is more pronounced for e_{31} that for e_{33}. The dilute model is an asymptotic limit of Mori–Tanaka model and doesn't have the compatibility with high limit concentration of inclusions ($f^I = 1$). It stays then unacceptable at the highest concentration of inclusions.

Fig. 5a shows the predicted numerical values of the piezoelectric strain constant d_{31} for long fibers ($c/a = 1000$). The composite used is PZT-5/epoxy-1. The predictions of the three models are nearly the

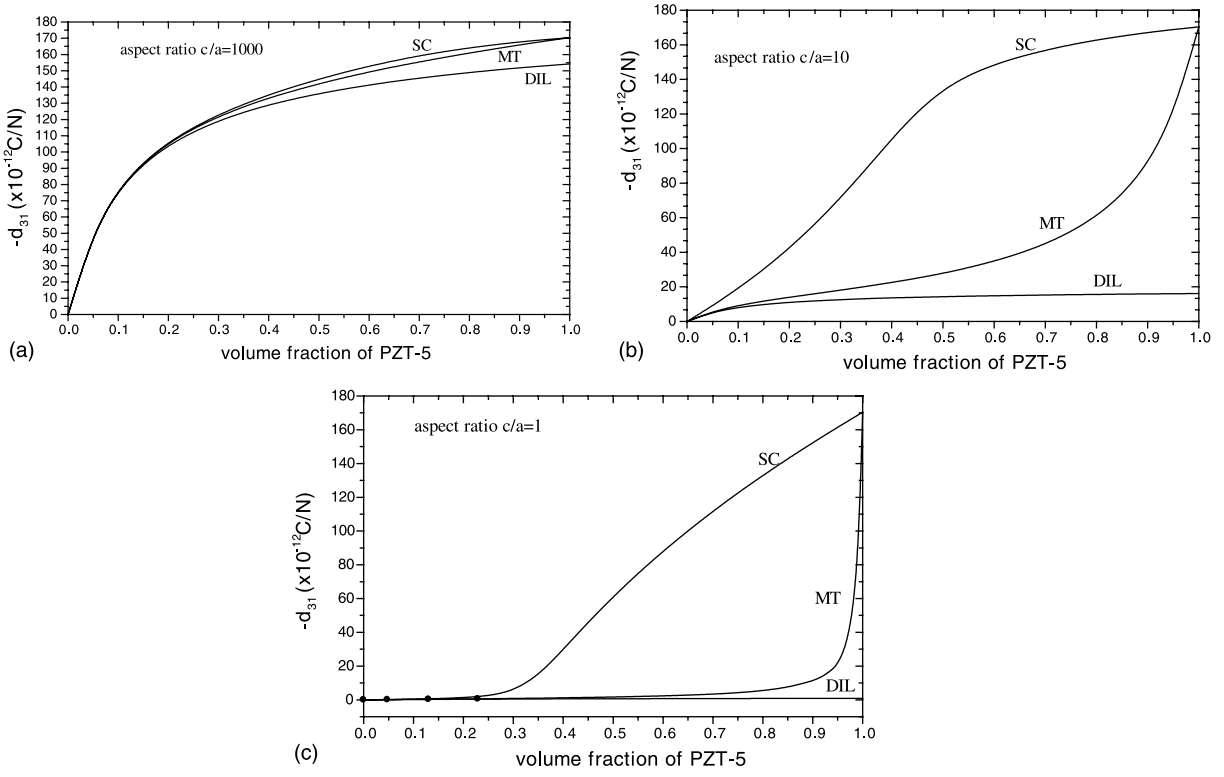

Fig. 5. (a) Effective piezoelectric module d_{31} predicted by the three micro-mechanical models of PZT-5 log fibers ($c/a = 1000$) reinforced epoxy composite as a function of fiber volume fraction. (b) Effective piezoelectric module d_{31} predicted by the three micro-mechanical models of PZT-5 for ellipsoidal ($c/a = 10$) reinforced epoxy composite as a function of fibers volume fraction. (c) Effective piezoelectric moduli d_{31} predicted by the three micro-mechanical models of PZT-5 for particles ($c/a = 1$) reinforced epoxy composite as a function of particles volume fraction. "●" Experimental results (Furukawa et al., 1976).

same but a big difference is shown for other shapes of inclusions. For ellipsoid (Fig. 5b) and particles (Fig. 5c), the self-consistent model overestimates the constant d_{31} over the volume fraction of inclusion equal to 0.2. The two other models give lowest values of d_{31} and agree well, for volume fraction low than 0.3, with limited experimental results of Furukawa et al. (1976) taken from a curve presented by Dunn and Taya (1993b). In light of these results, one can conclude that the self-consistent scheme leads to acceptable prediction of d_{31} only for concentrations less than 0.2 while the Mori–Tanaka's approach is in the best agreement with experimental results over that. As there is no available experimental results for large volume fractions of reinforcement, it can not be ascertained which prediction will be better at higher concentration.

Fig. 6 show the predicted evolution of effective piezoelectric coefficients e_{33} and e_h, defined by $e_h = e_{33} + 2e_{31}$, normalized by e_{33} and e_h of reinforcement, with aspect ratio of inclusions. The reinforcement is made of PZT-4 and the matrix of epoxy-2 (see Table 1). The inclusions volume fraction is fixed at 20% (Fig. 6a) and at 50% (Fig. 6b) respectively. It is clearly seen, as it was observed by Dunn and Taya (1993a) and Poizat and Sester (1999), that for the three numerical predictions, the geometry of reinforcement began affecting significantly the piezoelectric moduli of composite over the aspect ratio range of 5–50. At aspect ratio of approximately 100, the composite became saturated, and normalized piezoelectric constants do not increase or show an insignificant increasing. Additionally, for the reinforcement volume fraction of 50%, self-consistent model predicts overestimated results for spherical inclusions and gives the nearly same results as Mori–Tanaka and dilute approaches for the long fibers reinforcement.

In Fig. 7, normalized piezoelectric coefficient e_{33} and e_h for a fixed aspect ratio ($c/a = 1000$) are plotted versus the long fiber volume fraction of PZT-4. The matrix is an epoxy-2 matrix (see Table 1). Numerical results obtained by the three models are shown in Fig. 7. Results obtained by self-consistent and Mori–Tanaka models seem to be acceptable as they take the values 0 and 1 at low ($f^I = 0$) and high ($f^I = 1$) limit volume fractions. The results of the two models are nearly the same for normalized e_{33} for all volume fractions. Also for normalized e_h, for volume fraction low than 50%, the three models give the same results. The dilute approximation, even in this case, appears as asymptotic limit of the other approximations and take unacceptable values at high limit volume fraction ($f = 1$).

Using the possibility of the presented micro-mechanical methodology to treat all fiber orientations randomly distributed in epoxy matrix, Figs. 8 and 9, illustrate the evolution of effective piezoelectric coefficients d_{33} and d_{31} of PZT-7A/epoxy-1 composite with respect to volume fractions of fiber reinforcements

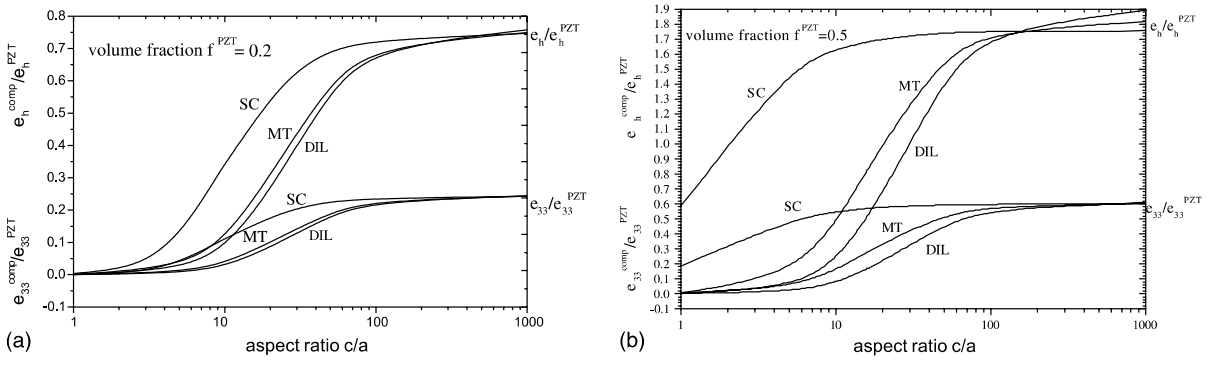

Fig. 6. (a) Piezoelectric coefficients e_{33} and $e_h = e_{33} + 2e_{31}$, normalized by e_{33} and e_h of PZT-4, as a function of particle aspect ratio for PZT-4 particle reinforced epoxy composite, computed by the three micro-mechanical models and at a fixed volume fraction of reinforcement $f = 0.2$. (b) Piezoelectric coefficients e_{33} and $e_h = e_{33} + 2e_{31}$, normalized by e_{33} and e_h of PZT-4, as a function of particle aspect ratio for PZT-4 particle reinforced epoxy composite, computed by the three micro-mechanical models and at a fixed volume fraction of reinforcement $f = 0.5$.

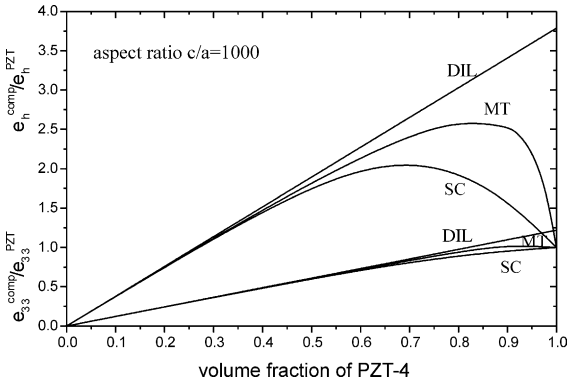

Fig. 7. Piezoelectric coefficients e_{33} and $e_h = e_{33} + 2e_{31}$, normalized by e_{33} and e_h of PZT-4, as a function of PZT-4 volume fraction for PZT-4 continuous fiber reinforced epoxy composite.

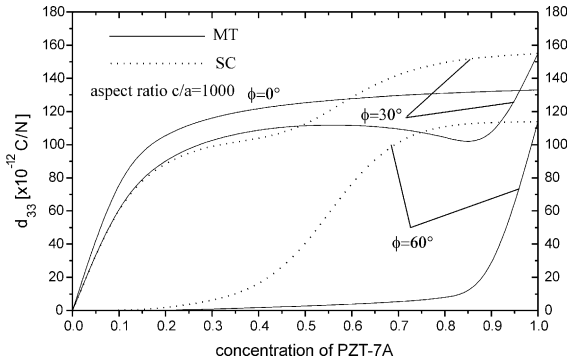

Fig. 8. Effective piezoelectric coefficient d_{33} of PZT-7A/epoxy composite predicted by Mori–Tanaka (MT) and self-consistent (SC) approaches for three orientations of fiber reinforcements ($\phi = 0°$, 30°, 60°).

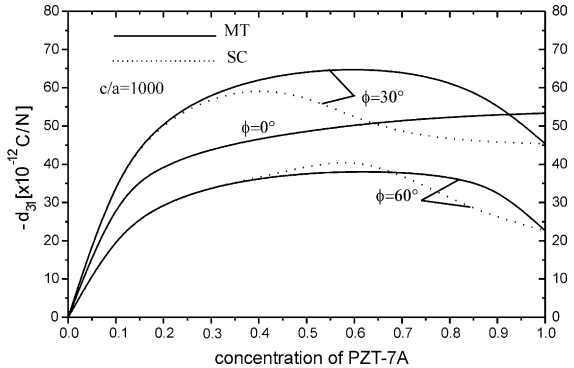

Fig. 9. Effective piezoelectric coefficient d_{31} of PZT-7A/epoxy for three orientations of fiber reinforcements ($\phi = 0°$, 30°, 60°).

for different orientations ϕ (Euler angle). Let us precise that in this analysis, the third axe of inclusion is kept respected with polling direction. For the orientation ($\phi = 0°$) and fiber inclusion, it was demonstrated, (Fig. 1), that all models lead to the same prediction for d_{33}. For ($\phi = 30°$), it can be shown from Fig. 8 that the self-consistent and Mori–Tanaka models give approximately the same result up to inclusion volume fraction ($f = 0.5$). But, the two predictions are completely different for more large inclusion volume fractions. The difference is more strong for ($\phi = 60°$). For d_{31} presented in Fig. 9, the two models lead to the same results for ($\phi = 0°$) and separate with each other for large inclusion volume fractions. This difference is more pronounced for ($\phi = 30°$). The coefficient d_{33} is highly sensitive to the orientation angles than d_{31}.

As the orientation angle of inclusions seems strongly affecting the predicted effective coefficients, a deep analysis of this influence will be presented in the next paper for various shapes and types on PZT inclusions.

6. Conclusion

In this paper, an electroelastic modeling for piezoelectric inclusions in an infinite non-piezoelectric matrix is presented. Analytical formulations of four electroelastic interaction tensors, related to Eshelby electroelastic tensors obtained by Dunn and Taya (1993a), are given for ellipsoidal inclusions. These tensors are basically used to derive the self-consistent model, Mori–Tanaka and dilute approaches. These tensors were obtained numerically based on Fourier's transforms and Gauss's integration. Using the obtained results, effective electroelastic moduli of piezoelectric multiphase composites are investigated by an iterative procedure in the context of self-consistent scheme. Generalized Mori–Tanaka's model and dilute approach are re-formulated and used in the analysis.

Namely, the presented micro-mechanics models are able to treat multiphase composites with reinforcement ranging from spherical particles to continuous long fibers randomly distributed at a fixed spatial orientations. Several examples of ceramic/epoxy composites have been investigated. Hence, it can be seen that self-consistent and Mori–Tanaka's methods lead to acceptable results with the fact that results obtained by the self-consistent method are over estimated than those of Mori–Tanaka's method. In contrast, the dilute approach leads to unacceptable results for large volume fractions and seems to be asymptotic limit of the above models. Numerical results show a strong dependence of effective electroelastic modulus on the volume fraction, aspect ratio and spatial orientation of reinforcement.

Acknowledgements

The second author wishes to acknowledge the assistance of the Fellowship grant from Fulbright and the opportunity to use the facility of Aerospace Engineering Department, Old Dominion University, Norfolk, VA, USA.

Appendix A

Since the expression (18) of the elastic displacement–electric potential U_K and the Eq. (17a) in this paper and using the fact that $G_{JK,i}(r - r') = -G_{JK,i'}(r - r')$, the elastic displacement and electric potential, U_K, can be expressed as follows:

$$U_K(r) = -\int_V E^0_{iJMn} G_{JK,i'n'}(r - r') U_M(r')\,\mathrm{d}V' \tag{A.1}$$

The partial derivative relations used are as follows:

$$\begin{aligned} G_{JK,i'n'}U_M &= (G_{JK,i'}U_M)_{,n'} - G_{JK,i'}U_{M,n'} \\ G_{JK,i'n'}U_M &= (G_{JK,i'}U_M)_{,n'} - (G_{JK}U_{M,n'})_{,i'} + G_{JK}U_{M,n'i'} \end{aligned} \tag{A.2}$$

Introducing (A.2) into (A.1) and using Stocks theorem, the expression of U_M becomes

$$U_K(r) = -\int_S E^0_{iJMn} G_{JK,i'} U_M n_{n'}\,\mathrm{d}S' + \int_S E^0_{iJMn} G_{JK} U_{M,n'} n_{i'}\,\mathrm{d}S' - \int_V E^0_{iJMn} G_{JK} U_{M,n'i'}\,\mathrm{d}V'$$

The first term of right hand side of the last equation is the elastic displacement-potential electric field in a homogeneous solid with equivalent geometry and boundary conditions as considered solid. This field will be denoted $U^0_K(r)$

In the other hand, the second integral can be expressed as

$$\int_S E^0_{iJMn} G_{JK} U_{M,n'} n_{i'}\,\mathrm{d}S' = \int_S G_{JK}\Sigma_{iJ} n_{i'}\,\mathrm{d}S' = \int_S G_{JK} T_J(r')\,\mathrm{d}S'$$

Σ_{iJ} is stress–electric displacement, n is the exterior normal of S and T_J is body force-electric charge. This integral vanishes because the boundaries conditions of the considered solid are only imposed elastic displacement–electric potential. (The solid is free of stress–electric displacement field.)

Finally $U_K(r)$ can be expressed as

$$U_K(r) = U^0_K(r) - \int_V E^0_{iJMn} G_{JK}(r - r') U_{M,n'i'}(r')\,\mathrm{d}V' \tag{A.3}$$

The substitution of the equation (16) of the paper into (A.3) leads to

$$U_K(r) = U^0_K(r) + \int_V G_{JK}(r - r')(\delta E_{iJMn}(r') U_{M,n}(r'))_{,i'}\,\mathrm{d}V'$$

Or, using strain-electric field Z_{Mn}

$$U_K(r) = U^0_K(r) + \int_V G_{JK}(r - r')(\delta E_{iJMn}(r') Z_{Mn}(r'))_{,i'}\,\mathrm{d}V' \tag{A.4}$$

Appendix B

B.1. The four interaction tensors T^{II}

B.1.1. Shorthand forms

$$T^{II}_{iJKl} = -\frac{1}{2}\int_{V^I}\int_{V^I} (G_{JK,li}(r - r') + G_{Jl,Ki}(r - r'))\,\mathrm{d}V'\,\mathrm{d}V \quad K = 1,2,3 \tag{B.1}$$

$$T^{II}_{iJKl} = -\int_{V^I}\int_{V^I} G_{JK,li}(r - r')\,\mathrm{d}V'\,\mathrm{d}V \quad K = 4 \tag{B.2}$$

B.1.2. Explicit forms

$$T^{II}_{ijkl} = \int_{V^I}\int_{V^I} -\frac{1}{2}\left(G_{jk,li}(r-r') + G_{jl,ki}(r-r')\right) \mathrm{d}V' \,\mathrm{d}V \quad J,K = 1,2,3 \tag{B.3}$$

$$T^{II}_{ikl} = \int_{V^I}\int_{V^I} -\frac{1}{2}\left(G_{4k,li}(r-r') + G_{4l,ki}(r-r')\right) \mathrm{d}V' \,\mathrm{d}V \quad J = 4,\ K = 1,2,3 \tag{B.4}$$

$$T^{II}_{ijl} = \int_{V^I}\int_{V^I} -G_{j4,li}(r-r') \,\mathrm{d}V' \,\mathrm{d}V \quad J = 1,2,3,\ K = 4 \tag{B.5}$$

$$T^{II}_{il} = \int_{V^I}\int_{V^I} -G_{44,li}(r-r') \,\mathrm{d}V' \,\mathrm{d}V \quad J = 4,\ K = 4 \tag{B.6}$$

The Green's four tensors signification is given in paper of Dunn (1994).

The computation of T^{II} is realized by Fourier's transforms of Green's functions.

Differential equation (17a), introduced in Section 3 of this paper, which are satisfied by Green's functions $G_{MK}(r-r')$ can be written in the following condensed form:

$$E_{iJMn}G_{JK,in}(r-r') + \delta_{MK}\delta(r-r') = 0$$

This leads to (Wang, 1992) and (Dunn, 1994)

$$E_{iJMn}\widetilde{G}_{JK}(q)q_n q_i = \delta_{MK} \tag{B.7}$$

B.2. Expression of T^{II} using the Fourier's transform of Green's functions

B.2.1. Spherical inclusion

In this case spherical inclusions with radius "q" equal at "a" is considered. In spherical system attached at the inclusion, the vector $\vec{q}$ became

$$q_p = q\chi_p \quad p = 1,2,3 \tag{B.8}$$

$$\vec{\chi} = \begin{cases} \sin\theta & \cos\varphi \\ \sin\theta & \sin\varphi \\ \cos\theta & \end{cases}$$

q, θ and φ are the spherical coordinates of the vector $\vec{q}$ defined in the following domains: $q \in [0,+\infty]$, $\theta \in [0,\pi]$ and $\varphi \in [0,2\pi]$ the introduction of the equations (B.8) into (B.7) leads to

$$E_{iJMn}\chi_n\chi_i(q^2\widetilde{G}_{JK}(q)) = \delta_{MK} \tag{B.9}$$

Let us introduce a matrix M defined by

$$M_{JM} = E_{iJMn}\chi_n\chi_i \tag{B.10}$$

The inverse matrix of M is then

$$M^{-1}_{JK} = q^2\widetilde{G}_{JK}(q) \tag{B.11}$$

The expression of T^{II}_{iJKl} in spherical coordinate system is given by

$$T^{II}_{iJKl} = \frac{a^3}{6}\int_0^{\pi} \sin\theta \,\mathrm{d}\theta \int_0^{2\pi} (\chi_i\chi_l q^2 \widetilde{G}_{JK} + \chi_i\chi_K q^2 \widetilde{G}_{Jl})\,\mathrm{d}\varphi \quad K = 1,2,3 \tag{B.12}$$

$$T^{II}_{iJKl} = \frac{a^3}{3}\int_0^{\pi} \sin\theta \,\mathrm{d}\theta \int_0^{2\pi} \chi_i\chi_l q^2 \widetilde{G}_{J4}\,\mathrm{d}\varphi \quad K = 4 \tag{B.13}$$

B.2.2. Ellipsoidal inclusion

An ellipsoidal inclusion with a, b and c as half axes is considered. The last combined vectors $\vec{r}$ and $\vec{q}$ are replaced into $\vec{R}$ and $\vec{Q}$ defined by

$$\vec{R}\begin{cases} R_1 = r_1 \\ R_2 = \frac{a}{b} r_2 \\ R_3 = \frac{a}{c} r_3 \end{cases} \quad \text{and} \quad \vec{Q}\begin{cases} Q_1 = q_1 \\ Q_2 = \frac{b}{a} q_2 \\ Q_3 = \frac{c}{a} q_3 \end{cases}$$

these vectors are expressed in principal system of inclusion.

The matrix relationship between $\vec{Q}$ and $\vec{q}$ is as follows:

$$q_i = \phi_{it} Q_t \tag{B.14}$$

with

$$[\phi] = \begin{bmatrix} 1 & 0 & 0 \\ 0 & \frac{a}{b} & 0 \\ 0 & 0 & \frac{a}{c} \end{bmatrix}$$

The expression of $\vec{Q}$ in this coordinate system is then

$$Q_t = Q\chi_t \tag{B.15}$$

Recall that

$$\vec{\chi} = \begin{cases} \sin\theta & \cos\varphi \\ \sin\theta & \sin\varphi \\ \cos\theta \end{cases}$$

The final expression of T^{II}_{iJKl} is then as the follows:

$$T^{II}_{iJKl} = \frac{a\cdot b\cdot c}{6}\int_0^{\pi} \sin\theta \,\mathrm{d}\theta \int_0^{2\pi} (\phi_{lt}\chi_t\phi_{iu}\chi_u Q^2 \widetilde{G}_{JK} + \phi_{Kt}\chi_t\phi_{iu}\chi_u Q^2 \widetilde{G}_{Jl})\,\mathrm{d}\varphi \quad K = 1,2,3 \tag{B.16}$$

$$T^{II}_{iJKl} = \frac{a\cdot b\cdot c}{3}\int_0^{\pi} \sin\theta \,\mathrm{d}\theta \int_0^{2\pi} \phi_{lt}\chi_t\phi_{iu}\chi_u Q^2 \widetilde{G}_{J4}\,\mathrm{d}\varphi \quad K = 4 \tag{B.17}$$

As in the case of spherical inclusion it can be introduce the matrix M defined by

$$Q^2 \widetilde{G}_{JK} = M^{-1}_{JK} \tag{B.18}$$

and

$$M_{JK} = E_{iJKl}\phi_{it}\phi_{lu}\chi_t\chi_u \tag{B.19}$$

Appendix C

Eqs. (34) and (35) of Section 4.2 lead to the following shorthand expression of concentration tensor A established for self-consistent method

$$A_{MnKl} = \left(I_{KlMn} + \frac{1}{V^I} T^{II}_{iJKl} \Delta E^I_{iJMn} \right)^{-1} \tag{C.1}$$

The inverse of A is then

$$A^{-1}_{KlMn} = I_{KlMn} + \frac{1}{V^I} T^{II}_{iJKl} \Delta E^I_{iJMn} \tag{C.2}$$

The Eq. (C.2) can be expressed using matrix notations as follows:

$$A^{-1}_{KlMn} = \begin{bmatrix} I_{klmn} & 0 \\ 0 & I_{ln} \end{bmatrix} + \frac{1}{V^I} \begin{bmatrix} T_{ijkl} & T_{ikl} \\ T_{ijl} & T_{il} \end{bmatrix} \begin{bmatrix} \Delta C_{ijmn} & \Delta e^t_{nij} \\ \Delta e_{imn} & -\Delta \kappa_{in} \end{bmatrix} \tag{C.3}$$

T_{ijkl}, T_{ikl}, T_{ijl}, T_{il} are the interaction tensors as shown in Appendix B. I_{klmn} and I_{ln} are the identity tensors of fourth and second orders respectively.

The term $T^{II}_{iJKl} \Delta E^I_{iJMn}$ is expressed with the following matrices:

$$T^{II}_{iJKl} \Delta E^I_{iJMn} = \begin{bmatrix} T^{\varepsilon}_4 & -T^E_3 \\ T^{\varepsilon}_3 & -T^E_2 \end{bmatrix} = \begin{bmatrix} T_{ijkl} & T_{ikl} \\ T_{ijl} & T_{il} \end{bmatrix} \begin{bmatrix} \Delta C_{ijmn} & \Delta e^t_{nij} \\ \Delta e_{imn} & -\Delta \kappa_{in} \end{bmatrix} \tag{C.4}$$

A simplified prescription of the matrices A_{MnKl} and I_{KlMn} are as

$$I_{KlMn} = \begin{bmatrix} I_4 & 0 \\ 0 & I_2 \end{bmatrix} \quad \text{and} \quad A_{MnKl} = \begin{bmatrix} A^{\varepsilon}_4 & A^E_3 \\ A^{\varepsilon}_3 & A^E_2 \end{bmatrix} \tag{C.5}$$

For the sake of clarity, the indices 4, 3 and 2 indicate the ranges of tensors and the prescription E and ε are introduced for distinguishing the different tensors. Considering the fact that $A^{-1} \cdot A = I$, (C.3)–(C.5) can be lead to matrices prescriptions

$$\begin{bmatrix} I_4 & 0 \\ 0 & I_2 \end{bmatrix} = \begin{bmatrix} I_4 + \frac{1}{V^I} T^{\varepsilon}_4 & -\frac{1}{V^I} T^E_3 \\ \frac{1}{V^I} T^{\varepsilon}_3 & I_2 - \frac{1}{V^I} T^E_2 \end{bmatrix} \times \begin{bmatrix} A^{\varepsilon}_4 & A^E_3 \\ A^{\varepsilon}_3 & A^E_2 \end{bmatrix} \tag{C.6}$$

The Eqs. (C.6) lead to the following expressions of the fourth concentration tensors:

$$A^{\varepsilon}_4 = \left[I_4 + \frac{1}{V^I} \left(T^{\varepsilon}_4 + \frac{1}{V^I} T^E_3 \left(I_2 - \frac{1}{V^I} T^E_2 \right)^{-1} T^{\varepsilon}_3 \right) \right]^{-1} \tag{C.7}$$

$$A^{\varepsilon}_3 = -\frac{1}{V^I} \left(I_2 - \frac{1}{V^I} T^E_2 \right)^{-1} T^{\varepsilon}_3 A^{\varepsilon}_4 \tag{C.8}$$

$$A^E_3 = \frac{1}{V^I} \left(I_4 + \frac{1}{V^I} T^{\varepsilon}_4 \right)^{-1} T^E_3 A^E_2 \tag{C.9}$$

$$A^E_2 = \left[I_2 - \frac{1}{V^I} \left(T^E_2 - \frac{1}{V^I} T^{\varepsilon}_3 \left(I_4 + \frac{1}{V^I} T^{\varepsilon}_4 \right)^{-1} T^E_3 \right) \right]^{-1} \tag{C.10}$$

Appendix D

Algorithm

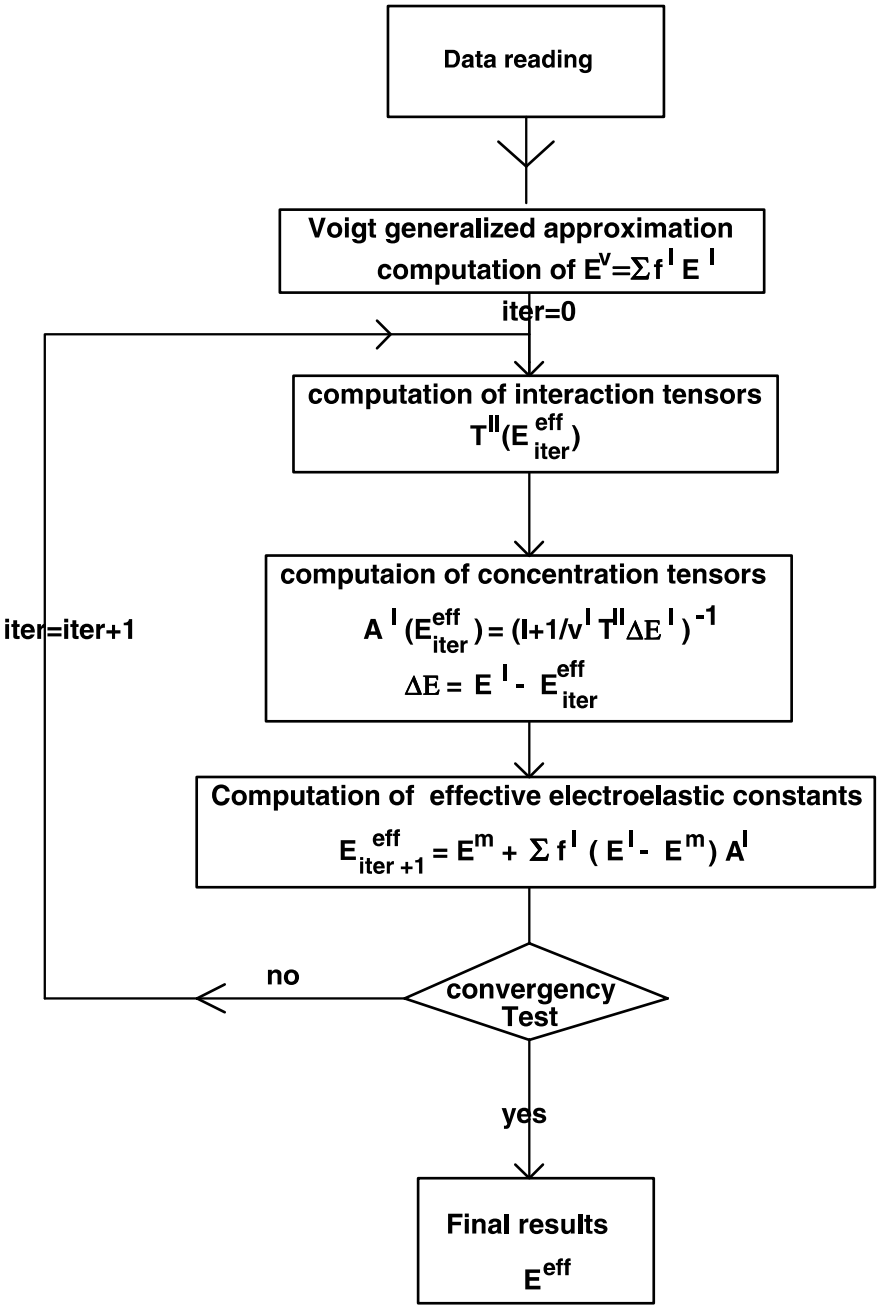

References

Banno, H., 1983. Recent developments of piezoelectric ceramic products and composites of synthetic rubber and piezoelectric ceramic particles. Ferroelectrics 50, 3–12.

Barnett, D.M., Lothe, J., 1975. Dislocations and line charges in anisotropic piezoelectric insolators, Phy. Status. Solidi. B 67, 105–111.

Benveniste, Y., 1992. The determination of the elastic and electric fields in piezoelectric inhomogeneity. J. Appl. Phys. 72 (3), 1086–1095.

Berlincourt, D.A., 1971. Piezoelectric crystals and ceramics. In: Mattiat, O.E. (Ed.), Ultrasonic Transducer Materials, pp. 63–119.

Challende, P., 1990. IEEE Trans. Ultrason. Ferroelect. Freq. Control 37, 135–140.

Chan, H.L.W., Unsworth, J., 1989. Simple model for piezoelectric ceramic/polymer 1–3 composites used in Ultrasonics Transducers applications. IEEE Trans. Ultrason. Ferroelect. Freq. Control 36, 434–441.

Chen, T., 1994. Micromechanical estimates of the overall thermoelectroelastic moduli of multiphase fibrous composites. Int. J. Solids Struct. 31, 3099–3111.

Dederish, P.H., Zeller, R., 1973. Z. Phys. 259, 103–113.

Deeg, W.F., 1980. The analysis of dislocation, crack and inclusion problems in piezoelectric solids. PhD dissertation, Stanford University, USA.

Dunn, M.L., Taya, M., 1993a. An analysis of piezoelectric composite materials containing ellipsoidal inhomogeneities. Proc. R. Soc. Lond. A 443, 265–287.

Dunn, M.L., Taya, M., 1993b. Micromechanics predictions of the effective electroelastic moduli of piezoelectric composites. Int. J. Solids Struct. 30 (2), 161–175.

Dunn, M.L., 1994. Electroelastic Green's functions for Transversely isotropic Piezoelectric media and their application to the solution of inclusion and inhomogeneity problems. Int. J. Eng. Sci. 32 (1), 119–131.

Dunn, M.L., Wienecke, H.A., 1997. Inclusions and inhomogeneities in transversely isotropic piezoelectric solids. Int. J. Solids Struct. 34 (27), 3571–3582.

Eshelby, J.D., 1957. The determination of the elastic field of an ellipsoidal inclusion, and related problems. Proc. R. Soc. Lond. A 241, 376–396.

Fakri, N., Azrar, L., 2001. Modeling of electroelastic behavior of piezoelectric medium—application to composite materials. In: Proceeding of Conference of Mechanics, Meknès, Morocco, Vol. 1, 71–72. In French.

Furukawa, T., Fujino, K., Fukada, E., 1976. Electromechanical properties in the composites of epoxy resin and PZT ceramics. Jpn. J. Appl. Phys. 15, 2119–2129.

Gaudenzi, P., 1997. On the electromechanical response of active composite materials with piezoelectric inclusions. Comput. Struct. 65 (2), 157–168.

Grekov, A.A., Karamarov, S.O., Kuprienko, A.A., 1989. Effective properties of a transversely isotropic piezocomposite with cylindrical inclusions. Ferroelectrics 99, 115–126.

Hershey, A.V., 1954. The elasticity of an isotropic aggregate of anisotropic cubic crystals. J. Appl. Mech. 21, 236–241.

Huang, J.H., 1995. Equivalent inclusion method for the work-hardening behavior of piezoelectric composites. Int. J. Solids Struct. 33, 1439–1451.

Huang, J.H., Kuo, W.-S., 1996. Micromechanics determination of the effective properties of piezoelectric composites containing spatially oriented short fibers. Acta Mater. 44 (12), 4889–4898.

Ikeda, T., 1990. Fundamentals of Piezoelectricity. Oxford University Press, Oxford.

Jiang, B., Fang, D.N., Hwang, K.C., 1999. A unified model for piezocomposites with non-piezoelectric matrix and piezoelectric ellipsoidal inclusions. Int. J. Solids Struct. 36, 2707–2733.

Kreher, W.S., 1998. Proceeding of the Euromech 373 Colloquium, Modelling and Control of adaptative Mech. Structures, ADAMES Preprint1/1998, pp. 21–30.

Kröner, E., 1958. Berechnung der elastischen konstanten des vielkristalls aus den konstanten einkristalls. Z. Phys. 151, 504–518.

Mikata, Y., 2001. Explicit determination of piezoelectric Eshelby tensors for a spheroidal inclusion. Int. J. Solids Struct. 38, 7045–7063.

Mori, T., Tanaka, K., 1973. Average stress in matrix and average elastic energy of materials with misfitting inclusions. Acta Metall. 21, 571–574.

Newnham, R.E., Skinner, D.P., Cross, L.E., 1978. Connectivity and piezoelectric-pyroelectric composites. Mater. Res. Bull. 13, 525–536.

Poizat, C., Sester, M., 1999. Effective properties of composites with embedded piezoelectric fibres. Comput. Mater. Sci. 16, 89–97.

Smith, W.A., 1989. The Role of piezocomposites in Ultrasonic Transducers, Proceeding of the IEEE 1989 Ultrasonic Symposium, 755–766.

Smith, W.A., Auld, B.A., 1991. Modelling 1–3 composite piezoelectrics: thickness-mode oscillation. IEEE Trans. Ultrason. Ferroelect. Freq. Control 38, 40–47.

Wang, B., Liu, Y., 1990. The average field in piezoelectric media with randomly distributed inclusions. In: Hsieh, R.K.T. (Ed.), Mechanical Modeling of New electromagnetic Materials. Elsevier, pp. 313–318.

Wang, B., 1992. Three-dimentional analysis of an ellipsoidal inclusion in a piezoelectric material. Int. J. Solids Struct. 29, 293–308.

Wang, B., 1994. Effective behaviour of piezoelectric composites. In: Ostoja-Starzevski, M., Jasiuk, I. (Eds.), Micromechanics of Random Media. Appl. Mech. Rev. 47, 112–121.